



UNIVERSITY OF NIŠ

The scientific journal **FACTA UNIVERSITATIS**

Series: **Mechanics, Automatic Control and Robotics** Vol.2, No 10, 2000 pp. 1177 - 1190

Editor of series: *Katica (Stevanovi)* Hedrih, e-mail: katica@masfak.masfak.ni.ac.yu

Address: Univerzitetski trg 2, 18000 Niš, YU, Tel: +381 18 547-095, Fax: +381 18 547-950

<http://ni.ac.yu/Facta>

DYNAMICS OF DOUBLE IMPACT OSCILLATORS

UDC 531.35+534.01(045)

František Peterka

Institute of Thermomechanics Academy of Sciences of the Czech Republic
Dolejškova 5, 182 00 Prague 8, Czech Republic
Phone:+420/2/66053083, FAX:+420/2/8584695, E-mail: peterka@it.cas.cz

Abstract. *The double impact oscillator represents two symmetrically arranged single impact oscillators. It is the model of a forming machine, which does not spread the impact impulses into its neighbourhood. The anti-phase impact motion of this system has the identical dynamics as the single system. The in-phase motion and the influence of asymmetries of the system parameters are studied using numerical simulations. Theoretical and simulation results are verified experimentally and the real value of the restitution coefficient is determined by this method.*

I. INTRODUCTION

The one-degree-of-freedom impact oscillator is one of the simplest strongly non-linear mechanical systems. It consists of an elastically suspended and periodically excited mass (cf. one half of Fig. 1), which can impact against a rigid stop. Its dynamics has been thoroughly investigated theoretically, experimentally and using simulation methods (see references in (Peterka and Vacík 1992) and (Peterka 1981)). The influence of the following parameters on the maximum velocity before impact during fundamental periodic impact motion was studied (Peterka 1981): coefficient of restitution, viscous and dry friction damping, static clearance, amplitude and frequency of the excitation force. This fundamental motion is practically most important and is characterised by the repetition of one impact in every period of the excitation force. There exist also other periodic and chaotic impact motions. Each motion has the region of existence and stability in the space of system parameters. Regions can mutually penetrate and create hysteresis subregions. Several regimes of the system motion exist there. Motion initial conditions (basins of attraction) or other conditions decide which motion will appear (see the set of papers in (Peterka and Vacík 1992, [16])).

Received May 26, 2000

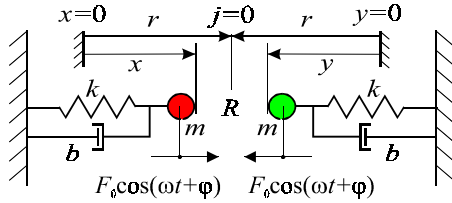


Fig. 1. Scheme of the double impact oscillator

Results obtained for the single oscillator are applicable for two symmetrically arranged impact oscillators – the double impact oscillator (Fig. 1), which can be considered as the model of a forming machine.

An advantage of such system, compared to the single impact oscillator, consists in the isolation of impact impulses from the neighbourhood of a forming machine and doubling of before-impact velocities.

The second degree of freedom introduces asymmetry into the system motion, which is undesirable for the application. Differences in initial conditions, driving forces or natural frequencies of subsystems cause other asymmetries. Constructional or assembly imperfections can also introduce asymmetries. It has been shown using numerical simulations and experiments, that small asymmetries do not affect the optimal operation of this system.

2. THEORETICAL ANALYSIS

The theoretical analysis will arise here from the differential equations of motion of the system. The solution of the simplest series of periodic impact motions and their stability is introduced in (Peterka and Vacík 1992) and (Peterka and Szöllös 1996) for the symmetric system without the viscous damping.

2.1 Symmetric Case

The impactless motion is described by the system of transformed differential equations

$$X'' + 2\beta X' + X = \cos(\eta\tau + \varphi), \tag{1}$$

$$Y'' + 2\beta Y' + Y = \cos(\eta\tau + \varphi), \tag{2}$$

where $X = x.k/F_0$, $Y = y.k/F_0$ and $\tau = \Omega t$ ($\Omega = \sqrt{k/m}$) are transformations of displacements and the time, respectively, $\eta = \omega/\Omega$ and $\beta = b/(2\sqrt{km})$ are the dimensionless frequency and viscous damping, respectively; $X' = dX/d\tau$, $X'' = d^2X/d\tau^2$.

Impacts occur, when the following condition is met

$$X + Y \geq 2\rho, \tag{3}$$

where $\rho = r.k/F_0$, is the dimensionless static clearance.

It is assumed that impacts are described by Newton's theory of impacts. Let X'_- , Y'_- and X'_+ , Y'_+ denote the before-impact and the after-impact velocities, respectively. Then:

$$X'_+ = [(1 - R) X'_- - (1 + R) Y'_-] / 2,$$

$$Y'_+ = [(1 - R) Y'_- - (1 + R) X'_-] / 2, \tag{4}$$

where $R = -(X'_+ + Y'_+)/ (X'_- + Y'_-)$ is the coefficient of restitution ($0 \leq R \leq 1$).

For plastic impacts ($R = 0$) have the masses equal after-impact velocities X'_p

$$X'_+ = -Y'_+ = (X'_- - Y'_-)/2 = X'_p \quad (5)$$

and there are two possibilities of the after-impact motion, according to the polarity of the after-impact relative acceleration $X''_+ + Y''_+$:

a) When the condition

$$X''_+ + Y''_+ \leq 0 \quad (6)$$

is met, then no forces press the masses together and the after-impact motion is described by Eqs. (1), (2) as for the motion with elastic impacts, when $X'_+ + Y'_+ \leq 0$.

b) When the condition (6) is not met, then the masses move together according to equation

$$J'' + 2\beta J' + J = 0, \quad (7)$$

with initial conditions

$$J(0) = X(\tau_i) - \rho \quad \text{and} \quad J'(0) = X'(\tau_i) = X'_p, \quad (8)$$

where τ_i is the instant of the plastic impact and J is the displacement of the masses from the centre ($j = 0$ in Fig. 1).

The time interval of such motion is named the after-impact dead zone of the masses relative motion. It ends at the instant τ_e , when the press force F_p disappears. This force is proportional to the fictive positive acceleration $X''_+ + Y''_+$, which is evaluated during numerical simulation of the motion (Fig. 2(a)).

The motion is described then by Eqs. (1), (2) with initial conditions

$$\begin{aligned} X(0) &= J(\tau_e) + \rho, & Y(0) &= -J(\tau_e) + \rho; \\ X'(0) &= -Y'(0) = J'(\tau_e) \end{aligned} \quad (9)$$

The motion of the system with asymmetric initial conditions, plastic impacts and after-impact dead zones is introduced in Fig. 2. Figure 2(a) shows, that polarity of force F_p (condition (6)) decides about the after-impact dead zone and its duration. The first plastic impact does not meet the condition for the joined motion of masses after impact. Dead zones appear after remaining three impacts. The motion of the general impact-dry-friction pair of bodies is described in more detail in (Peterka 1999).

2.1.1. Transformation of the system coordinates

The transformation of coordinates X, Y into coordinates U, V , according to Eqs.

$$U = X + Y, \quad V = X - Y, \quad (10)$$

introduce clear view of the double impact oscillator behaviour. U and V are coordinates of the anti-phase and in-phase motion of the system, respectively. This transformation is introduced in (Landa 1996). Equations (1), (2) are transformed into Eqs.

$$U'' + 2\beta U' + U = 2 \cos(\eta \tau + \varphi), \quad U'_+ = -R U'_-, \quad (11)$$

$$V'' + 2\beta V' + V = 0, \quad V'_+ = V'_-, \quad (12)$$

It follows from Eq. (11), that anti-phase motion corresponds to the single impact

oscillator motion with double excitation force amplitude. The in-phase motion (Eq. (12)) is the free damped vibration, which introduces the asymmetry into the system motion. The presence of viscous damping eliminates this asymmetry, as it seen in Fig. 2(b). Therefore the symmetric impact motion gradually stabilises.

It follows from this analysis, that all known results obtained for the simple impact oscillator describe the behaviour of the symmetric motion of the double impact oscillator, but before-impact velocities should be doubled.

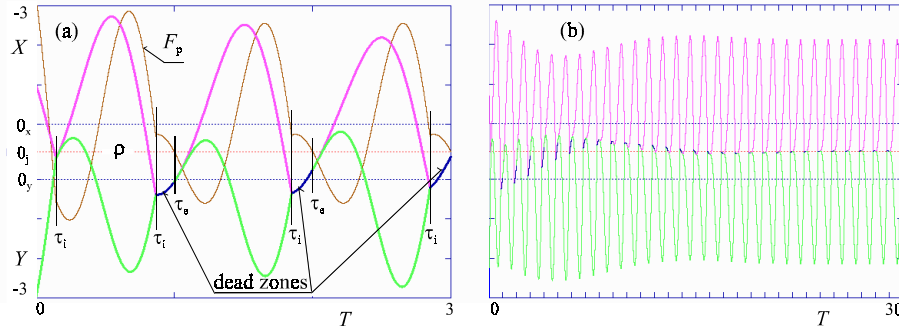


Fig. 2. Time series of motion during 3 and 30 excitation periods T with asymmetric initial conditions $X(0) = -1, X'(0) = 1.5, Y(0) = -3, Y'(0) = 2.5, \varphi = \pi/4$ and dimensionless parameters $\eta = 0.95, \beta = 0.1, \rho = 0.7$ and $R = 0$

2.1.2. Regions of existence of different impact motions in the plane of parameters ρ, η

The dimensionless frequency η and static clearance ρ are important parameters of the system, which decide about the regime of motion. Therefore the regions of existence and stability of motions are usually evaluated in plane η, ρ . The map of regions of motions with plastic impacts, is shown in Fig. 3, for example.

Regions are labelled by the quantity $z = p/n$, which denotes the mean number of impacts in one excitation period T (p and n are the number of impacts and the number of periods T in the impact motion period, respectively). The value $z = 1_j$ or 2_j means, that during the $z = 1$ or $z = 2$ impact motion appears after impact dead zones (see Fig. 2 for the motion $z = 1_j$). Values $z = 0 \div 1$ and $z = 0 \div 2$ denote regions of the periodic subharmonic and chaotic impact motions, which are named regions of beat impact motions.

The region of impactless motion ($z = 0$) is bounded by grazing boundaries ρ' , where a certain impact motion should arise. Boundaries ρ' are identical with the amplitude-frequency characteristics of the impactless motion. The region of the periodic one-impact motion without after-impact dead zone ($z = 1$) is bounded by the period-doubling stability boundary s_1 , where the system motion transits into the beat motion region between boundaries ρ' and s_1 . Region $z = 1$ is also bounded by the saddle-node stability boundaries s_2 , where one-impact motion suddenly transits into impactless motion. Therefore two responses ($z = 0$ or $z = 1$) of the system exist in regions between boundaries ρ', s_2 , named the hysteresis regions. The region of the one-impact motion with after-impact dead zones ($z = 1_j$) is bounded from below by the boundary $\rho_p = -1$, where the dead zone increases to the whole excitation period T , because $F_p = F_0$. The impact motion vanishes and

masses remain joined all the time in the static position ($j = 0$ in Fig. 1).

The system motion with plastic impacts is described in more detail in (Peterka and Szöllös 1996).

2.1.3. Bifurcation diagrams

The evaluation of the motion characteristics, e. g. along the section q of existence and stability regions in Fig. 3, offers a deeper view of the system motion behaviour. The quasi-stationary amplitude characteristics $X_m(\eta)$ and the before-impact velocity characteristics $(X'+ Y')(\eta)$ are shown in Fig. 4. They were simulated numerically at increasing and decreasing frequency η (see arrows along characteristics). Figure 4 contains also time series and phase trajectories of typical motions, which exist along line q in Fig. 3 ($z = 0$ for $\eta = 0.8$ and $\eta = 1.2$, $z = 1/2$ for $\eta = 0.87$ and $z = 1$ for $\eta = 1$).

The impactless motion transits in point G_1 into a narrow interval η of chaotic impact motion. Then the periodic impact motions $z = 2/4$, $z = 1/2$ and $z = 1$ gradually stabilise. The fundamental $z=1$ motion is stable in the interval η between points S_1, S_2 – points of stability boundaries s_1, s_2 (Fig. 3). The impactless motion, which arises in point S_2 , slowly loses the component of a free vibration for the sake of very small value $\beta = 0.002$ of the viscous damping. The frequency η decreases from the value $\eta = 1.4$ up to point G_2 , where the $z = 1$ impact motion suddenly appears again. The extreme E of before-impact velocities exists in the hysteresis region between points G_2, S_2 . This extreme regime can be attained by the quasi-stationary increase of frequency η from the region of the definite system response $z = 1$. If the extreme frequency $\eta = 1.19$ is constant, then it is necessary to choose the motion initial conditions from the basin of attraction of $z = 1$ motion, for its definite stabilisation.

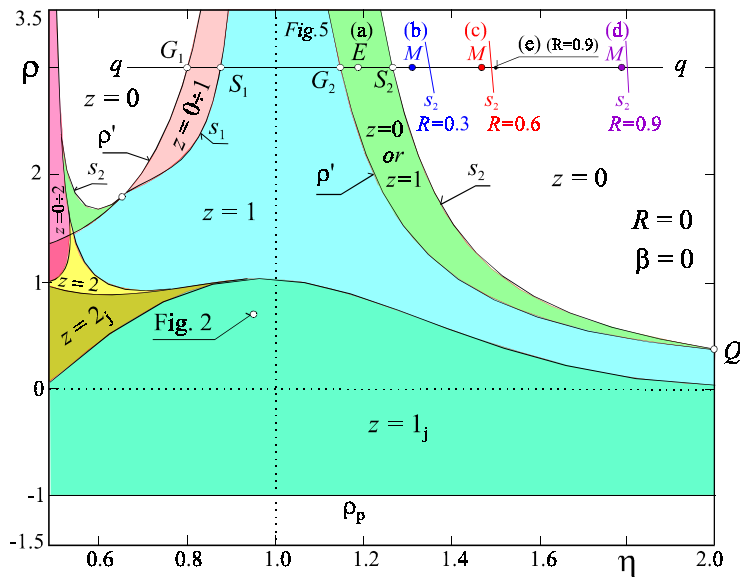


Fig. 3. Regions of existence and stability of motions with plastic impacts

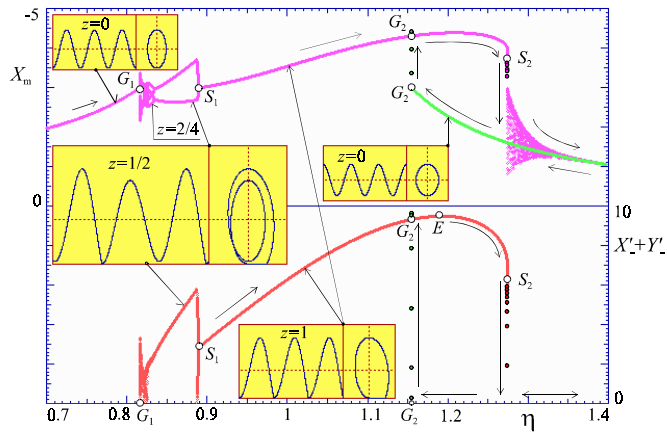


Fig. 4. Bifurcation diagrams and trajectories of motions along line q in Fig. 3

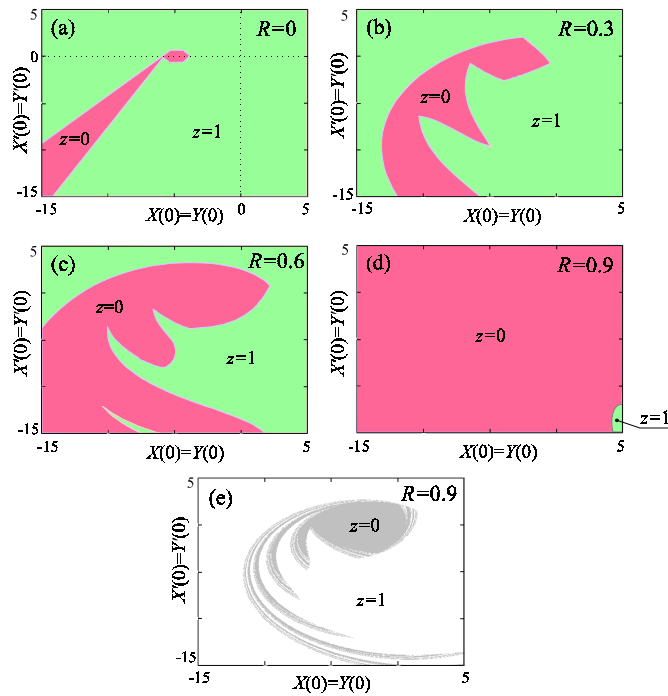


Fig. 5. Basins of attraction of the impact motion ($z = 1$) and impactless motion ($z = 0$) for parameters $\rho=3$, $\beta=0.02$ and $\varphi=0$ for different coefficients of restitution R
 (a) $R = 0$, $\eta = 1.19$, $(X' + Y')_{\max} = 9.26$; (b) $R = 0.3$, $\eta = 1.31$, $(X' + Y')_{\max} = 9.53$
 (c) $R = 0.6$, $\eta = 1.47$, $(X' + Y')_{\max} = 11.9$; (d) $R = 0.9$, $\eta = 1.78$, $(X' + Y')_{\max} = 28.16$
 (e) $R = 0.9$, $\eta = 1.5$, $X' + Y' = 13.65$

2.1.4. *Basins of attraction of different motions in regions with manifold response of the system*

The basin of attraction of the $z = 1$ impact motion in point E is shown in Fig. 5(a). It was obtained under the assumption that $\varphi = 0$ and initial conditions of both subsystems are identical. The basin of attraction of impactless ($z = 0$) motion is very small, so the periodic motion with plastic impacts can be attained simply, e.g. from the zero initial conditions. It has been shown in (Peterka and Szöllös 1996), that it does not depend on the initial phase φ of the excitation forces.

When the impacts become elastic and the coefficient of restitution R increases from zero to one, then regions of impact motions become more complex (see e. g. Figs. 8, 11). Hysteresis regions, as well as beat motion regions, enlarge. Fig. 3 shows it schematically along line q for the hysteresis region. All stability boundaries s_2 shift right and touch the grazing bifurcation boundary p' in point Q . Points of the before-impact velocity extremes, denoted by M for $R=0.3, 0.6, 0.9$ in Fig.3, similarly shift and approach more and more the stability boundaries s_2 . Therefore it is more and more difficult to attain these optimal regimes by the choice of motion initial conditions. This is graphically expressed in Figs. 5(a) – (d). Figure 5 shows also basins of attraction (e) in the centre of the hysteresis region of the almost elastic impact motion ($R = 0.9$).

2.2. Asymmetric Cases

Asymmetries in the double oscillator can considerably influence, in general, the system behaviour. Asymmetries of

- 1) motion initial conditions,
- 2) amplitudes of driving forces,
- 3) natural frequencies

are considered as an example.

ad 1) The oscillations become symmetric for asymmetric initial conditions, when viscous friction is present. When viscous friction is missing, then the initial asymmetry preserves in spite of a considerable amount of energy losses during impacts as has been discussed in Chap. 2.1.1.

ad 2) Asymmetry of the driving forces amplitudes introduces a systematic asymmetry of the motion, as follows from the transformation (10) of motion coordinates.

If a difference of 5% between excitation force amplitudes is assumed, then the differential equations of motion

$$\begin{aligned} X'' + 2\beta X' + X &= \cos(\eta\tau + \varphi) \\ Y'' + 2\beta Y' + Y &= 0.95 \cos(\eta\tau + \varphi) \end{aligned} \quad (13)$$

are transformed into

$$\begin{aligned} U'' + 2\beta U' + U &= 1.95 \cos(\eta\tau + \varphi) \\ V'' + 2\beta V' + V &= 0.05 \cos(\eta\tau + \varphi) \end{aligned} \quad (14)$$

and the in-phase motion component V is present all the time.

ad 3) Let us consider the equations of motion

$$\begin{aligned} X'' + 2\beta X' + X &= \cos(\eta\tau + \varphi) \\ Y'' + 2\beta Y' + 0.95 Y &= \cos(\eta\tau + \varphi), \end{aligned} \quad (15)$$

which express 2.5% asymmetry of natural frequencies. These equations are transformed into

$$U'' + 2\beta U' + U = 2 \cos(\eta \tau + \varphi) + 0.025(U - V), \quad V'' + 2\beta V' + V = -0.025(U - V). \quad (16)$$

It follows from Eqs. (16), that anti-phase and in-phase components of the system motion cannot be separated and the motion asymmetry preserves again.

The influence of asymmetries on the optimum impact regime of the system (Fig. 4) has been investigated using bifurcation diagrams in the frequency interval $0.9 < \eta < 1.4$ (Fig. 6). The comparison of the behaviour of asymmetric systems (Figs. 6(c) – (f)) with the symmetric case (Figs. 6(a), (b)) shows, that small asymmetries do not influence especially the before-impact velocity $X'_- + Y'_-$ in the neighbourhood of the optimal frequency η , which corresponds to points E .

The asymmetry manifests itself through resonance phenomena near the resonance ($\eta = 1$) of the impactless motion of the single oscillator (see Figs. 6(c), (e) and 6(f)) and it is more emphatic on the motion amplitude characteristics, than on the before-impact velocity characteristics.

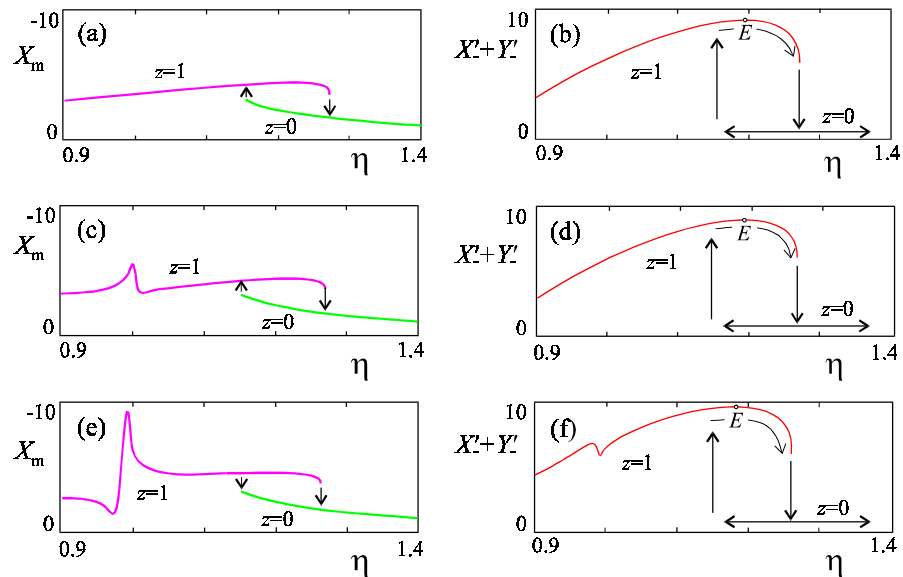


Fig. 6. Frequency characteristics of the optimal impact motion ($z = 1$) and impactless motion ($z = 0$) for the symmetric subsystems (a), (b), asymmetric exciting force amplitudes (c), (d) and natural frequencies (e), (f)

3. SIMULATIONS

Thirty years ago, analogue simulations allowed to obtain fundamental knowledge of the impact oscillator dynamics (Peterka 1974), (Irie et al. 1974). The current numerical simulations offer more extensive both qualitative and quantitative investigations. The program NON-1-SIM (Peterka and Formánek 1994) has been prepared, especially for the investigation of the single impact oscillator dynamics and it can be used also for

educational purposes. The program NON-1-SIM shows the introductory picture (Fig. 7(a)), which explains in more detail the application possibility of this program. It consists from two parts.

The *Information* part contains ten groups 0–9 of problems, which can be solved. Each of groups is supplemented by its own picture (see e. g. picture 8 in Fig. 7(b), explaining one of roads from the periodic subharmonic impact motion into the chaotic motion).

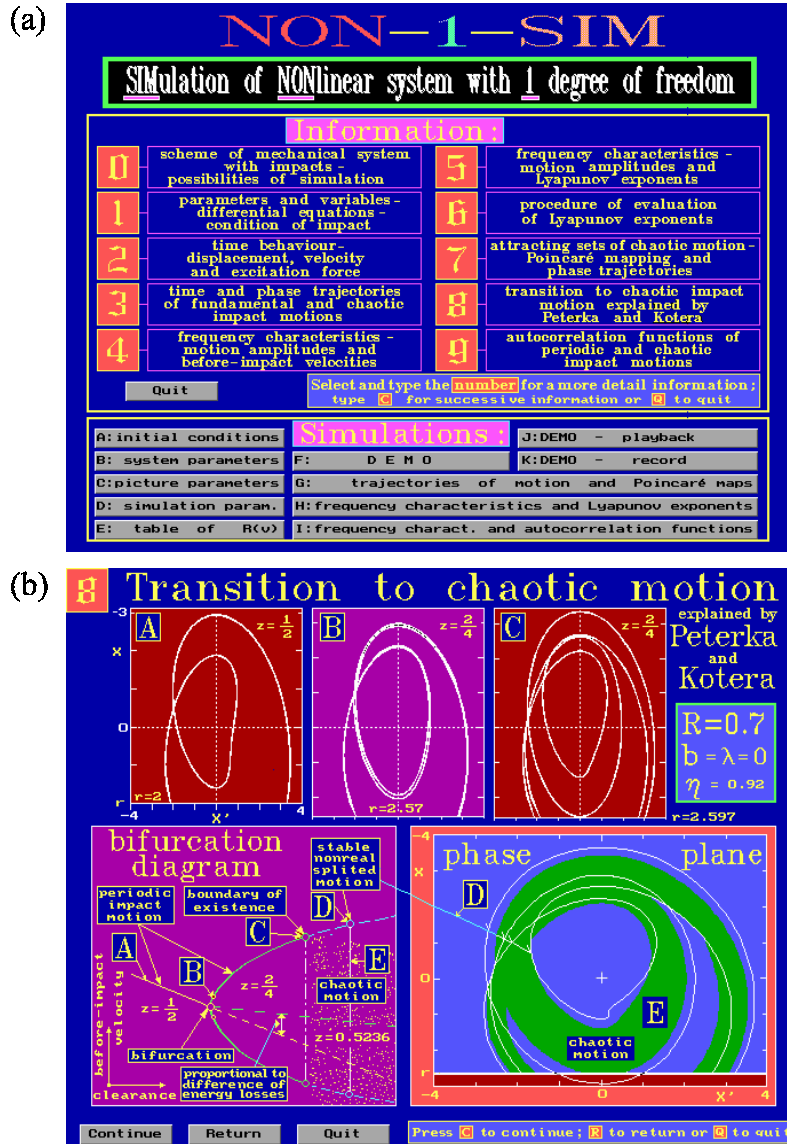


Fig. 7. Study pictures of the NON-1-SIM programme of numerical simulations of the impact oscillator motion

The *Simulation* part contains five buttons *A–E*, which can determine 38 values of initial conditions, system's parameters, picture's parameters, simulation parameters and the table of the dependence $R(v)$ of the coefficient of restitution on the before-impact velocity X' . (R can be also constant or analytically defined).

There exist three simulation procedures. The procedure *G* simulates and displays time series, phase trajectories and Poincarè maps of the system motion. The dimensionless clearance ρ and the excitation frequency η can be interactively changed from the keyboard. The same possibility have both procedures *H*, *I*, which simulate the frequency or clearance characteristics ($X_m(\eta)$, $X_m(\rho)$, $X'(\eta)$, $X'(\rho)$), as well as Lyapunov exponents and autocorrelation functions. Pictures can be supplemented by trajectories of the impact oscillator motion, as it is shown in Fig. 4. Procedure *I* can simulate also usual amplitude- and phase-frequency characteristics of the impactless motion.

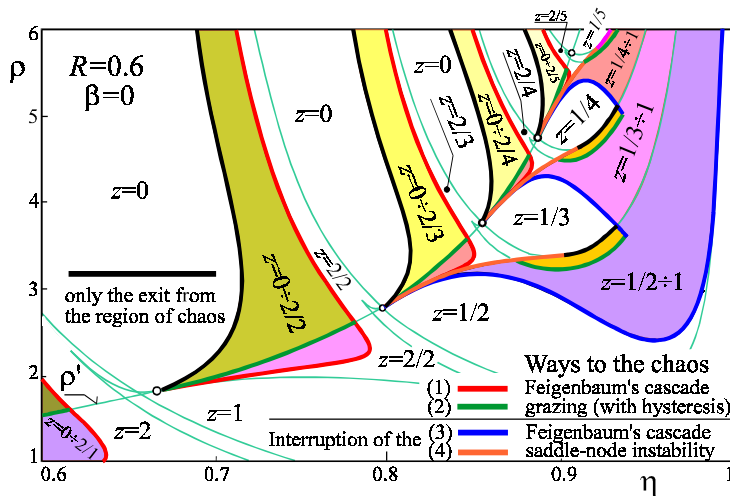


Fig. 8. Input and output boundaries of chaotic motion regions

The NON-1-SIM program offers the authors DEMO versions of mentioned simulation procedures, which explain in more detail the simulation possibilities and can be executed by the button *F*. The user can record own DEMO version of procedures, using button *K*, and execute them by button *J*.

Boundaries of stability and existence regions (see e. g. Figs. 3, 8, 11) have very diverse character and it is difficult to create a general program for their simulation. Therefore different bifurcation boundaries should be evaluated interactively during the simulation.

Figure 8 shows, as an example, the diversity of boundaries of the chaotic impact motion regions. Four input boundaries (1)–(4) characterise different ways into the chaos. Three of them, (2)–(4), are specific to the impact motion. Ways (3) and (4) are caused by additional impacts, which appear during the development of the period-doubling and saddle-node instability of periodic subharmonic impact motions. The way (3) is shown in Fig. 7(b) and the system behaviour along all boundaries is described in (Peterka and Kotera 1996) and (Peterka 1997).

4. EXPERIMENT

The experimental setup of the double impact oscillator is shown in Fig. 9. Its scheme and block scheme of electronic equipment controlling and evaluating the motion are given in Fig. 10. Masses 1 are clamped using blade springs 2 to traversable frames 5, which carry also vibrators 4 (LSD V201). These vibrators excite masses by rods 3. The static clearance $2r$ is set up by the right-left screw 6 axially fixed to the foundation 7. Computer 10 determines both frequency and amplitude of harmonic signal of the generator 12 (H&P 3324A). 13 are amplifiers LDS PA25E. Vibrations are measured by accelerometers 8 (B&K 4366) and integrating circuits 14 (RFT 036). The velocity of one mass is measured by the laser vibrometer 15 (POLYTEC OFV-302). One mass is electrically isolated and impacts switch on the circuit of the DC supply 16 (TESLA BS-525) for their indication. The computer stores measured signals during the time interval 1s by the 16-channel-AD converter 11 (National Instruments AT-MIO-16E-10), which samples signals with frequency 2 kHz. The natural frequency and viscous damping of separated systems are $\Omega = 12.6$ Hz, $\beta = 0.07$.

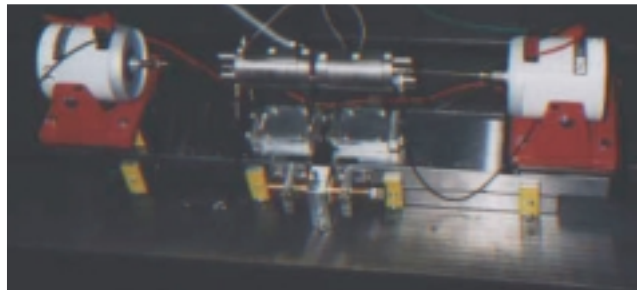


Fig. 9. Mechanical model of double impact oscillator

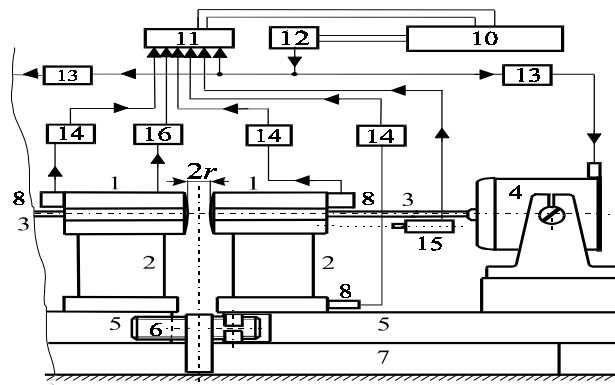


Fig. 10. Scheme of experimental equipment

5. COMPARISON OF RESULTS OF NUMERICAL SIMULATIONS AND EXPERIMENTS

The results are compared by regions of existence of different system motions in the plane ρ, η (Fig. 11, where regions of all evaluated impact motions are denoted by a value of the impact number z) as well as by numerically simulated trajectories and experimentally

measured quantities of typical periodic and chaotic impact motions (Figs. 12, 13). Figure 13 shows also the vibrations of the frame 5 (Fig. 10), which are of the order of μm and without impact impulses.

The real value of restitution coefficient $R = 0.9$ of impacting bodies was determined by the simulation of stability boundary s_2 according to the experimentally obtained boundary s_2 , because the course of boundary s_2 depends expressively on R (see Chap. 2.1.4 and Fig. 3).

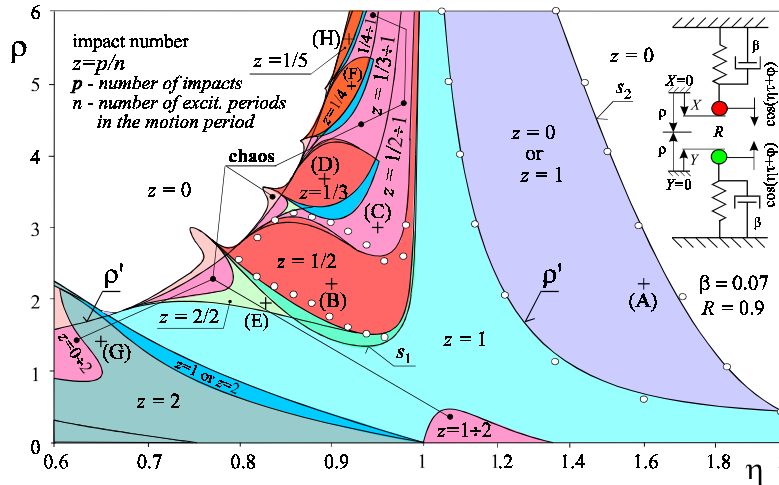


Fig. 11. Regions of impact motions simulated and experimentally verified.

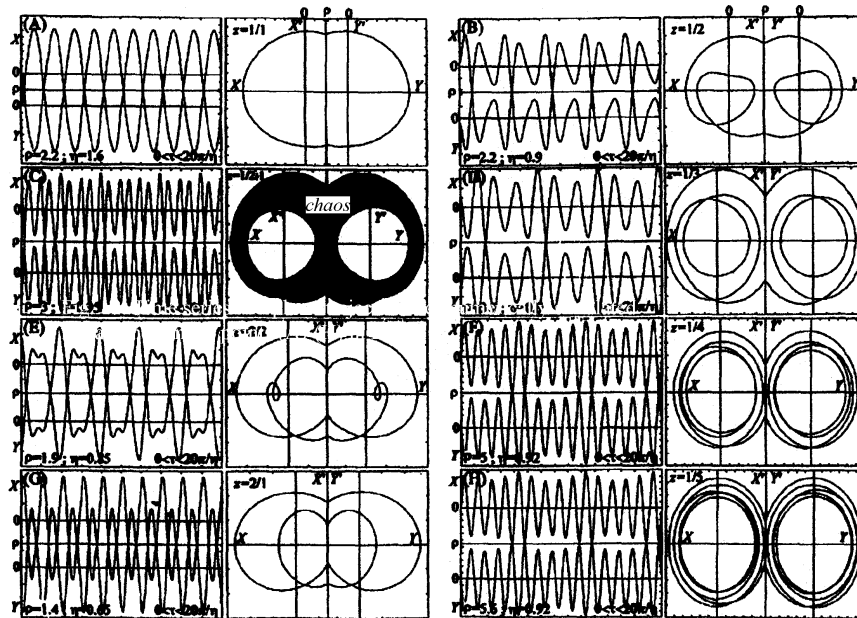


Fig. 12. Time series and phase trajectories of numerically simulated impact motions in points (A)–(H) in Fig. 11.

There exist a series of $z = 1/n$ -impact motions. Five of them ($n = 1 \div 5$) are shown in Figs. 12(A), (B), (D), (F), (H) and 13(A), (B), (D), (F), (H), corresponding to points (A), (B),(D),(F),(H) in Fig. 11. Impact motions $n \geq 2$ create one of groups of periodic subharmonic impact motions. Figures 11 – 13 contain, for example, also the periodic $z = 2/2$ impact motion (point (E)), which is one of other subharmonic motions. It arises by splitting of the $z = 1$ motion.

The first motion from the group of more impact motions $z = p/n$ ($p \geq 2, n = 1$) is shown in Figs. 12(G) and 13(G). The chaotic impact motion $z = 1/2 \div 1$ is in Figs. 12(C), 13(E).

Experimentally ascertained regions have the same structure as those attained numerically, but boundaries are shown only in a limited number of points denoted by circles along the hysteresis region of $z = 0$ and $z = 1$ motions and along the $z = 1/2$ region. The agreement of numerical and experimental results is very good.

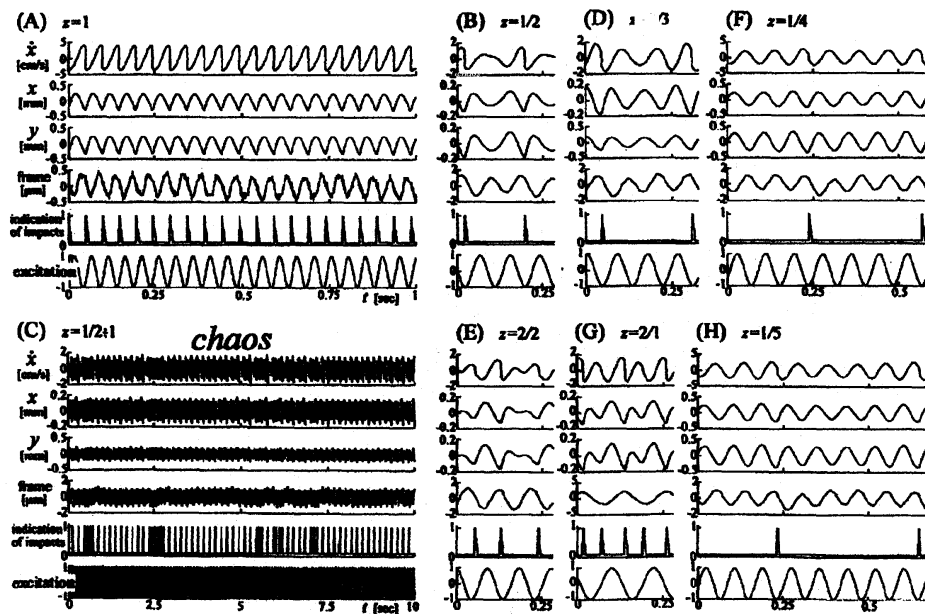


Fig. 13. Time series of experimentally obtained impact motions in points (A)–(H) in Fig. 11.

6 CONCLUSION

The correctness of the mathematical model of the double impact oscillator and the numerical simulation of its motion has been successfully verified experimentally. The value of the restitution coefficient can be determined accurately using both methods. Experiments confirmed also former results of the theoretical analysis and the simulation of the single impact oscillator dynamics with respect to regions of periodic and chaotic motions and their structure in dependence on the static clearance ρ and excitation frequency η .

REFERENCES

1. Irie, T., Yamada, G., Matsuzaki, H., 1974, *On the Dynamic Response of a Vibro-Impact System to Random Force*, Bulletin of the Faculty of Engineering, Hokkaido University, No.72, pp. 13-24.
2. Landa, P. S., 1996, *Nonlinear Oscillations and Waves in Dynamical Systems*, Kluwer Academic Publishers.
3. Peterka, F., 1974, *Laws of Impact Motion of Mechanical Systems with One Degree of Freedom. Patr II – Results of Analogue Computer Modelling of the Motion*, Acta Technica ČSAV, No.5, pp. 569-580.
4. Peterka, F., 1981, *Introduction to Oscillations of Mechanical Systems with Internal Impacts*, ACADEMIA, Prague, 269 p. (in Czech).
5. Peterka, F., 1997, *Dynamics of the Impact Oscillator*, Proceedings, IUTAM Symposium on New Applications of Nonlinear and Chaotic Dynamics in Mechanics, Ithaca, NY, USA, 27 July – 1 August 1996, Kluwer Academic Publishers.
6. Peterka, F., 1999, *Analysis of Motion of the Impact-Dry-Friction Pair of Bodies and its Application to the Investigation of the Impact Dampers Dynamics*, ASME 1999 Design Engineering Technical Conferences, MOVIC'99, Session "Friction and Impact Induced Vibrations", paper DETC99/ VIB-8350, Las Vegas, USA, September 12-15, 1999.
7. Peterka, F., Formánek, P., 1994, *Simulation of Motion with Strong Nonlinearities*, Proceedings, CISS - First Joint Conference of International Simulation Societies, ETH Zurich, Switzerland, August 22 - 25, 1994, pp. 137-141.
8. Peterka, F., Kotera, T., 1996, *Four Ways from Periodic to Chaotic Motion in the Impact Oscillator*, Machine Vibration 5, pp. 71-82, Springer-Verlag London Limited.
9. Peterka, F., Szöllös, O., 1997, *Dynamics of the Opposed Pile Driver*, Proceedings, IUTAM Symposium on Interaction between Dynamics and Control in Advanced Mechanical Systems, Eindhoven, The Netherlands, April 21-26, 1996, Kluwer Academic Publishers, Dordrecht, The Netherlands, pp. 271-278.
10. Peterka, F., Szöllös, O., 1996, *The Stability Analysis of a Symmetric Two-Degree-of-Freedom System with Impacts*, Proc., EUROMECH - 2nd European Nonlinear Oscillations Conference, Prague, Sept. 9 – 13, 1996, ČVUT.
11. Peterka, F., Vacík, J., 1992, *Transition to Chaotic Motion in Mechanical Systems with Impacts*, Journal of Sound and Vibration, 154(1), pp. 95-115.

DINAMIKA DVOUDARNIH OSCILATORA

František Peterka

Oscilator sa obostranim sudarom je mehanički sistem sa jednim stepenom slobode čija se masa periodično pobuđuje. Istraživanje njegovog ponašanja počelo je pedesetih. Newton-ova elementarna teorija sudara je obično smatrana modelom sudara. Fundamentalni zakoni kretanja sistema su danas poznati kao rezultat dubokih teorijskih i simulacionih istraživanja i oni su verifikovani eksperimentima. Svi rezultati su primenljivi i za anti-fazno kretanje oscilatora dvostrukog sudara, koji ima veliki značaj u oblikovanju sečenju itd.

Interes istraživanja je usresređen na dinamiku oscilatora sa mekim sudarom, kada se trajanje sudara ne može zanemariti a disipativne sile između tela u sudaru su izabrane prema realnoj situaciji. Kelvin-Voigt-ov model sudara je primenjen u prvom koraku ove studije. Kada se zaustavna krutost menja od nule do beskonačnosti tada se simulira prelaz od linearnog (bez sudara) kretanja do strogo nelinearnog kretanja sa krutim sudarom. Dinamika oba granična slučaja je poznata i sada je takođe poznat i razvoj nelinearnih svojstava kretanja kada se tvrdoća sudara raste. Ovde će biti objašnjena dinamika oscilatora sudara. Biće prikazani i video zapisi analogne i numeričke simulacije, kao i eksperimenti. Osnovna struktura članka je sledeća: teorijska analiza, eksperiment i dinamika oscilatora sa mekim sudarom.